Density-functional study of the structure and stability of ZnO surfaces

B. Meyer and Dominik Marx
Lehrstuhl für Theoretische Chemie, Ruhr-Universität Bochum, 44780 Bochum, Germany
(Received 27 June 2002; revised 23 October 2002; published 9 January 2003; publisher error corrected 15 January 2003)

An extensive theoretical investigation of the nonpolar $(10\bar{1}0)$ and $(11\bar{2}0)$ surfaces as well as the polar zinc-terminated (0001)-Zn and oxygen-terminated $(000\bar{1})$-O surfaces of ZnO is presented. Particular attention is given to the convergence properties of various parameters such as basis set, *k*-point mesh, slab thickness, or relaxation constraints within local-density and generalized-gradient approximation pseudopotential calculations using both plane-wave and mixed-basis sets. The pros and cons of different approaches to deal with the stability problem of the polar surfaces are discussed. Reliable results for the structural relaxations and the energetics of these surfaces are presented and compared to previous theoretical and experimental data, which are also concisely reviewed and commented.

DOI: 10.1103/PhysRevB.67.035403 PACS number(s): 68.35.Bs, 81.05.Dz, 68.47.Gh

I. INTRODUCTION

The II-VI semiconductor ZnO has become a frequently studied material in surface science because of its wide range of technological applications. ZnO is a basic material for varistors, thyristors, and optical coatings. In addition, its direct band gap makes it an interesting candidate for blue and UV light-emitting diodes and laser diodes.[1] The electronic and structural properties of the ZnO surfaces are, in particular, important in its applications as chemical sensor in gas detecting systems and as catalyst for hydrogenation and dehydrogenation reactions. In combination with Cu particles at the surface, ZnO is a selective and efficient catalyst for the methanol synthesis,[2] where it is employed in industrial scale. The mechanism behind the enhanced catalytic activity when combined with Cu is poorly understood. However, before this interesting interplay between the ZnO substrate and the Cu particles can be addressed, a thorough understanding of the underlying clean ZnO surfaces is necessary.

From a physical/chemical point of view, ZnO is a very interesting material because of the mixed covalent/ionic aspects in the chemical bonding. ZnO crystallizes in the hexagonal wurtzite structure ($B4$), which consists of hexagonal Zn and O planes stacked alternately along the *c*-axis (see Fig. 1). Anions and cations are fourfold coordinated, respectively, like in the closely related zinc-blende structure. A tetrahedral coordinated bulk structure is typical for rather covalent semiconductors. On the other hand, ZnO shows great similarities with ionic insulators such as MgO.[3] This is why ZnO is often called the ''ionic extreme'' of tetrahedral coordinated semiconductors.

Wurtzite crystals are dominated by four low Miller index surfaces: the nonpolar $(10\bar{1}0)$ and $(11\bar{2}0)$ surfaces and the polar zinc-terminated (0001)-Zn and oxygen-terminated $(000\bar{1})$-O surfaces (see Fig. 1). By ion sputtering and annealing at not too high temperatures, all four surfaces can be prepared in a bulk terminated, unreconstructed state, where the surface atoms only undergo symmetry conserving relaxations. A typical $p(1\times1)$ pattern is observed in low-energy electron diffraction (LEED) and other diffraction experiments.[4–8] Although in a recent He-scattering experiment[9] it was shown that O-terminated $(000\bar{1})$ surfaces with $p(1\times1)$ LEED patterns are usually hydrogen covered whereas the clean O-terminated surface exhibits a (3×1) reconstruction, we will focus in this study on the clean, unreconstructed surfaces of ZnO.

In the present paper, we investigate all four main crystal terminations of ZnO. The fully relaxed geometric structures and the surface/cleavage energies have been calculated using a first-principles density-functional theory (DFT) method. We have employed both, a local-density approximation (LDA) and a generalized-gradient approximation (GGA) functional. We will discuss the relative stability of the four surfaces and how the surface relaxations of the nonpolar faces are connected to the covalency/ionicity of the chemical bond in ZnO. Finally, a detailed comparison with existing theoretical and experimental results will be given.

The nonpolar $(10\bar{1}0)$ surface of ZnO has been the focus of several experimental and theoretical studies. However, the form of the relaxation of the surface atoms is still very controversial. Duke *et al.*[5] concluded from their best LEED analysis[10] that the top-layer zinc ion is displaced downwards by $\Delta d_{\perp}(\mathrm{Zn}) = -0.45 \pm 0.1$ Å and likewise the top-layer oxygen by $\Delta d_{\perp}(\mathrm{O}) = -0.05 \pm 0.1$ Å, leading to a tilt of the Zn-O dimer of $12° \pm 5°$. No compelling evidence for lateral distortions within the first layer or for second-layer relaxations were obtained, but small improvements could be achieved by assuming a lateral displacement of the Zn ion toward oxygen by $\Delta d_{\parallel}(\mathrm{Zn}) = 0.1 \pm 0.2$ Å.[11] The strong inward relaxation of the Zn ion was later confirmed by Göpel *et al.*[12] in an angle-resolved photoemission experiment. By comparing the relative position of a particular surface state with its theoretically predicted geometry dependence, a Zn displacement downwards by $\Delta d_{\perp}(\mathrm{Zn}) = -0.4$ Å was concluded.

In contrast, Jedrecy *et al.*[13] found best agreement with their grazing incidence x-ray diffraction (GIXD) data for a structural model where the top-layer zinc atom is displaced downwards by only $\Delta d_{\perp}(\mathrm{Zn}) = -0.06 \pm 0.02$ Å and shifted toward oxygen by $\Delta d_{\parallel}(\mathrm{Zn}) = 0.05 \pm 0.02$ Å. However, for their samples they observed a high density of steps and from their best-fit model they predict rather high vacancy concen-

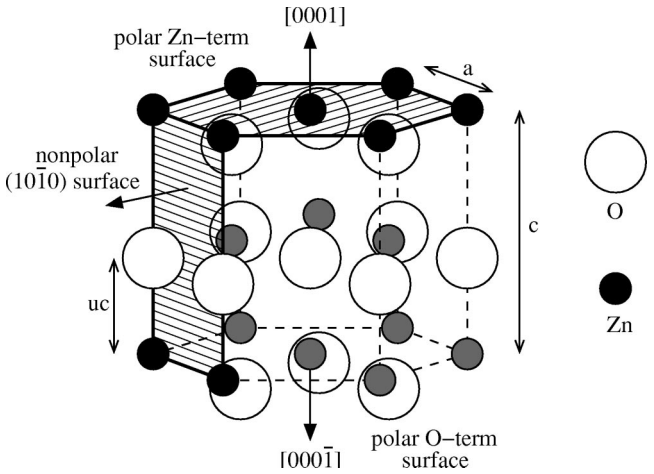

FIG. 1. Wurtzite structure ($B4$) of ZnO with the polar zinc-terminated (0001)-Zn, the polar oxygen-terminated (000$\bar{1}$)-O, and the nonpolar (10$\bar{1}$0) surfaces.

trations in the first two surface layers with occupancy factors of 0.77 ± 0.02 and 0.90 ± 0.04 for the first and second layer, respectively. On the other hand, Parker *et al.*[14] reported scanning tunneling microscopy images of the nonpolar (10$\bar{1}$0) surfaces with atomic resolution, where large flat terraces are found and no defects are visible in areas as large as 11×14 surface unit cells. Due to the small scattering contribution, the position of oxygen could not be determined very accurately in the GIXD experiment of Ref. 13. The result of the best fit was that O relaxes further toward the bulk than Zn with $\Delta d_{\perp}(\mathrm{O})=-0.12\pm0.06$ Å. This would be very unusual, since to our knowledge no (10$\bar{1}$0) wurtzite or (110) zinc-blende surface structure has been reported where the surface dimers tilts with the cation above the anion.

The first theoretical investigations of the (10$\bar{1}$0) surface were done using empirical tight-binding (TB) models. With two very different TB models, Wang and Duke[15] found a strong displacement of $\Delta d_{\perp}(\mathrm{Zn})=-0.57$ Å, whereas Ivanov and Pollmann[16] obtained an almost bulklike surface geometry. A recent calculation with atomistic potentials based on a shell model[17] predicted $\Delta d_{\perp}(\mathrm{Zn})=-0.25$ Å and a rather strong upward relaxation of the second-layer Zn of $+0.165$ Å.

Several *ab initio* studies (DFT-LDA,[18] Hartree-Fock (HF),[19] and a hybrid HF and DFT method using the B3LYP functional[20]) employing Gaussian orbitals as basis functions to solve the electronic structure problem favor small inward relaxations of Zn and small tilts of the ZnO-dimers of 2° to 5°. However, it is questionable if these studies represent fully converged results. There is only one recent first-principles DFT-LDA calculation using plane waves[21] where larger relaxations with a tilt of 11.7° were obtained.

The nonpolar (11$\bar{2}$0) ZnO surface has been less frequently studied than its (10$\bar{1}$0) counterpart. The two tight-binding models[15,16] predicted the same relaxation behavior for the (11$\bar{2}$0) as for the (10$\bar{1}$0) surface: Wang and Duke[15] found a strong zinc displacement of $\Delta d_{\perp}(\mathrm{Zn})=-0.54$ Å toward the bulk whereas the TB model of Ivanov and Pollmann preferred an almost bulklike surface structure. With a first-principles hybrid B3LYP method, Wander and Harrison[22] found much smaller relaxations for the (11$\bar{2}$0) surface than for the (10$\bar{1}$0) face, but not all degrees of freedom were relaxed in this study. To our knowledge there has been no quantitative experimental investigation.

Coming to the polar surfaces, we encounter the fundamental problem that in an ionic model these surfaces are unstable and should not exist. They are so-called ''Tasker type-3'' surfaces,[26] and with simple electrostatic arguments it can be shown that the surface energy diverges for such a configuration.[26] To stabilize the polar surfaces, a rearrangement of charges between the O- and the Zn-terminated surfaces needs to take place, in which the Zn-terminated side becomes less positively charged and the O-terminated face less negative. In fact, most polar surfaces show massive surface reconstructions or exhibit facetting to accommodate the charge transfer.[8] Also randomly distributed vacancies, impurity atoms in the surface layers, or the presence of charged adsorbates are possible mechanisms to stabilize polar surfaces. However, the polar ZnO surfaces are remarkably stable, and many experiments suggest that they are in an unreconstructed, clean, and fully ordered state.[8] Despite many investigations how the polar ZnO surfaces are stabilized is still an open question.[8]

Assuming clean and unreconstructed surfaces, the reduction in surface charge density can only occur from a redistribution of the electrons. Negative charge has to be transferred from the O-terminated face to the Zn-terminated side, leading to partially occupied bands at the surface. This so-called metallization of the surface has been used by all previous *ab initio* calculations[8,27,28] to model the polar ZnO surfaces and will also be employed in the present study. However, whether or not the surfaces are metallic will depend on the width of the partially occupied bands.

Several attempts have been made to determine the layer relaxations of the unreconstructed polar surfaces. In an early dynamical LEED analysis Duke and Lubinsky[7] found an outer Zn-O double-layer spacing of $d_{12}=0.607$ Å for the Zn-terminated surface and $d_{12}=0.807$ Å for the O-terminated face. Unfortunately, this analysis was based on an early bulk structure of ZnO, see Ref. 29, in which the bulk double-layer spacing was assumed to be 0.807 Å instead of 0.612 Å.

For the Zn-terminated surface, it was concluded from the comparison of x-ray photo-diffraction (XPD) data with scattering simulations[30] that any inward relaxation of the surface Zn layer can be ruled out. Coaxial impact-collision ion-scattering spectroscopy[31] proposed an expansion of d_{12} by $+0.35$ Å. Also an expansion of d_{12} by $+0.05$ Å for the Zn-terminated surface was found in a GIXD measurement.[32] In this experiment, the x-ray data could best be fitted by assuming a random removal of 1/4 of the Zn atoms in the surface layer. On the other hand, from the shadowing and blocking edges of a low-energy alkali-metal ion scattering[33] (LEIS) experiment, no evidence for substantial quantities of point defects in the Zn-terminated as well as in the O-terminated surface was found.

For the O-terminated surface, it was concluded from LEIS

(Ref. 33) that the Zn-O double-layer spacing d_{12} is close to its bulk value. An XPD study[34] found a contraction of 25% of d_{12}, but like in the LEED analysis,[7] the wrong bulk structure of Ref. 29 was used in the scattering simulations. A GIXD measurement[32] predicted also an inward relaxation of the topmost O layer by -0.33 Å and an outward relaxation of the underlying Zn plane by $+0.08$ Å. The occupancy probabilities were fitted, resulting in 1.3 and 0.7 for the first bilayer O and Zn, respectively. After considerably improved sample preparation was achieved, the same authors reinvestigated the O-terminated polar surface.[35] Best agreement with their GIXD data was now found for a structural model where both the upper O and Zn planes relax inwards by -0.19 ± 0.02 Å and -0.07 ± 0.01 Å, respectively, with occupancy factors of 1.0 in the oxygen plane and 0.75 ± 0.03 in the underlying Zn plane. The inward relaxation of the O-layer has been confirmed by another surface x-ray diffraction measurement,[27] where $\Delta d_{12}=-0.24\pm0.06$ Å and $\Delta d_{23}=+0.04\pm0.05$ Å was obtained.

Ab initio calculations on polar slabs[27,28,8] predict, consistently for both surface terminations, contractions for the first Zn-O double-layer distance, with a larger inward relaxation at the O-terminated surface.

In view of the above-discussed discrepancies between different experimental and theoretical investigations, it is our aim to provide a consistent set of fully converged calculations for the four main ZnO surfaces. We attempt to overcome the restrictions of previous theoretical studies such that the current study can be regarded as a reference for perfectly ordered, defect-free surfaces. An accurate set of uniform theoretical data may then allow us to discuss the differences between theory and experiment in terms of deviations between the model of ideal, unreconstructed surfaces as assumed in the *ab initio* simulations and the structure of the surfaces occurring in nature. In particular, for the polar surfaces this may give insight into how these surfaces are stabilized.

II. THEORETICAL DETAILS

A. Method of calculation and bulk properties

We have carried out self-consistent total-energy calculations within the framework of the DFT.[36] The exchange and correlation effects were treated within both, the LDA (Refs. 37 and 38) and the GGA, where we used the functional of Perdew, Burke, and Ernzerhof[39] (PBE).

Two different pseudopotential schemes were applied: For the study of the nonpolar surfaces we used pseudopotentials of the Vanderbilt ultrasoft type.[40] The electronic wave functions were expanded in a plane-wave basis set including plane waves up to a cutoff energy of 25 Ry. A conjugate gradient technique as described in Ref. 41 was employed to minimize the Kohn-Sham total-energy functional.

For the calculations on the polar surfaces we used norm-conserving pseudopotentials[42] together with a mixed-basis set consisting of plane waves and nonoverlapping localized orbitals for the O $2p$ and the Zn $3d$ electrons.[43] A plane-wave cutoff energy of 20 Ry was sufficient to get well-converged results. To improve convergence in the presence of partly occupied bands, a Gaussian broadening[44] with a smearing parameter of 0.1 eV was included. For several configurations representing nonpolar surfaces we repeated the calculations with the mixed-basis approach. No significant differences compared to the results from the ultrasoft-pseudopotential method could be seen.

TABLE I. Computed and experimental values of the structural parameters for bulk ZnO. a and c are the lattice constants, u is an internal coordinate of the wurtzite structure which determines the relative position of the anion and cation sublattice along the c axis, B_0 is the bulk modulus, and p_T is the transition pressure between the wurtzite ($B4$) and rocksalt ($B1$) structure of ZnO. Experimental values are from Refs. 23–25. Relative deviations from experiment are given in parentheses.

	LDA	PBE	Expt.
a(Å)	3.193 (−1.7%)	3.282 (+1.0%)	3.250
c(Å)	5.163 (−0.8%)	5.291 (+1.6%)	5.207
c/a	1.617	1.612	1.602
u	0.3783	0.3792	0.3825
B_0 (GPa)	161	128	143
p_T (GPa)	9.0	11.8	9.0−9.5

It is a well-known shortcoming of LDA and GGA that both predict the Zn d bands to be roughly 3 eV too high in energy as compared to experiment.[12,45] In consequence, the Zn d states hybridize stronger with the O p valence bands, thereby shifting them unphysically close to the conduction band. The underestimate for the band gap is therefore even more severe in ZnO than in other semiconductors. In our calculations we obtained band gaps of 0.78 eV and 0.74 eV with LDA and PBE, respectively, as opposed to the experimental value of 3.4 eV. The band gap and the position of the Zn-d bands can be improved significantly if a self-interaction correction (SIC) is used.[38] Usually SIC calculations are very demanding, but if the SIC effects are incorporated into the pseudopotential,[46] the additional calculational cost is modest. Unfortunately, the SIC pseudopotential scheme does not improve the structural properties of ZnO (Ref. 46) and also causes problems when accurate atomic forces are needed.[47] Therefore we have omitted the use of SIC pseudopotentials in our calculations.

The computed structural parameters for bulk ZnO are shown in Table I. Mixed-basis and ultrasoft-pseudopotential calculations give the same results within the accuracy displayed in Table I. As is typical for the functionals, LDA underestimates the lattice constants by 1–2 %, and GGA overestimates them by roughly the same amount. The c/a ratio strongly influences the internal parameter u. If $u=1/4+a^2/3c^2$, all nearest-neighbor bonds are equal. Since the c/a ratio is slightly overestimated in our calculations, we get u values that are slightly smaller than observed in experiment.

The construction of appropriate supercells for the study of the surfaces will be detailed in the following section. All atomic configurations were fully relaxed by minimizing the atomic forces using a variable-metric scheme.[48] Convergence was assumed when the forces on the ions were less than 0.005 eV/Å.

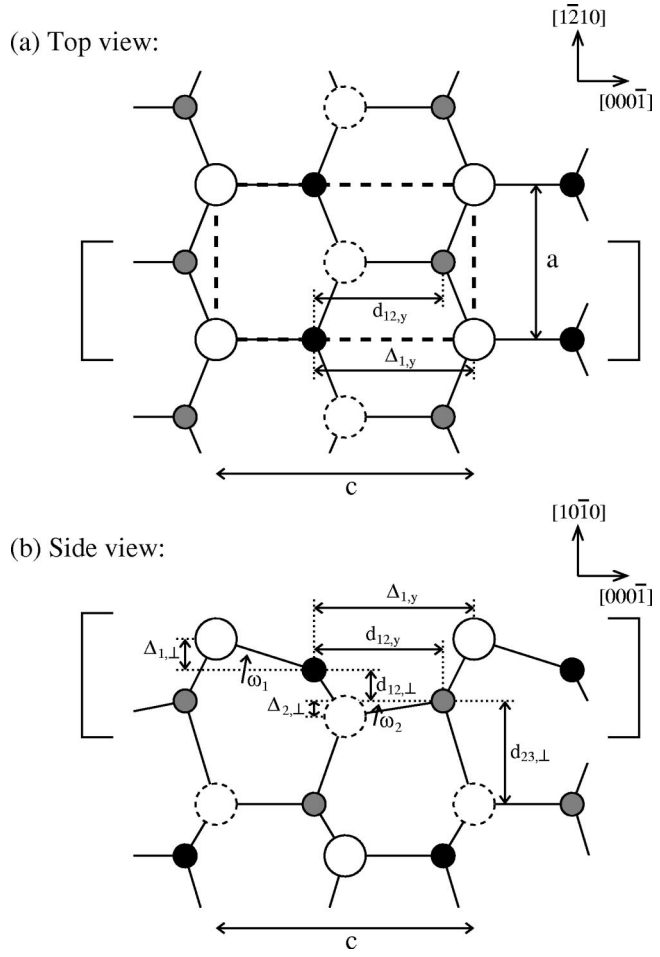

FIG. 2. Schematic diagram of the surface geometry and the independent structural parameters of the nonpolar $(10\bar{1}0)$ surface. The brackets indicate the two atomic layers shown in top and side view. Open and filled symbols are the O and Zn ions, respectively, and the solid lines represent nearest-neighbor bonds. The atoms in the first layer are shown by solid/black, second-layer atoms by dashed/shaded circles. The surface unit cell is indicated by dashed lines.

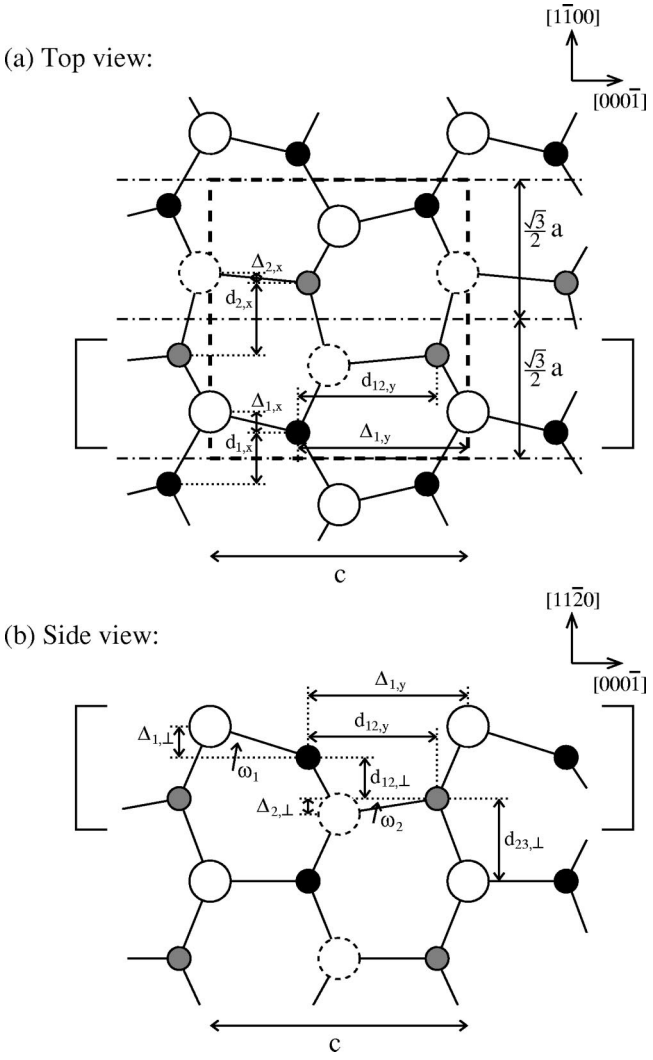

FIG. 3. Schematic top and side view of the surface geometry of the nonpolar $(11\bar{2}0)$ surface. The same representation as in Fig. 2 is used. The glide planes are indicated by dashed-dotted lines.

B. Surfaces, slab structures, and the stability problem

All surfaces were represented by periodically repeated slabs consisting of several atomic layers and separated by a vacuum region of 9.4–12.4 Å. For the polar surfaces a dipole correction[49,50] was used to prevent artificial electrostatic interactions between the repeated units. To simulate the underlying bulk structure, the slab lattice constant in the direction parallel to the surface was always set equal to the theoretical equilibrium bulk value (see Table I).

The nonpolar surfaces are obtained by cutting the crystal perpendicular to the hexagonal Zn and O layers (see Fig. 1). In both cases, for the $(10\bar{1}0)$ and the $(11\bar{2}0)$ planes, two equivalent surfaces are created so that always stoichiometric slabs with the same surface termination on top and at the bottom can be formed.

The $(10\bar{1}0)$ surface geometry is sketched in Fig. 2. Each surface layer contains one ZnO dimer. The dimers form characteristic rows along the $[1\bar{2}10]$ direction which are separated by trenches. Slabs with 4–20 atomic layers were used, thus containing up to 40 atoms, and the Brillouin zone of the supercell was sampled with a $(4\times2\times2)$ Monkhorst-Pack[51] *k*-point grid. No differences were found when going to a $(6\times4\times2)$ mesh.

The surface layers of the $(11\bar{2}0)$ surface are built up by two ZnO dimers, which form zigzag lines along the surface (see Fig. 3). The two dimers are equivalent and are related by a glide plane symmetry. This symmetry is not destroyed by the atomic relaxations of the surface.[6] The slabs in our calculations were built of four to eight atomic layers with up to 32 atoms, and a $(2\times2\times2)$ Monkhorst-Pack[51] *k*-point mesh was used. Again, a denser $(4\times4\times2)$ mesh did not alter the results.

Cleaving the crystal perpendicular to the *c* axis (see Fig. 1) always creates simultaneously a Zn- and an O-terminated polar (0001) and $(000\bar{1})$ surface, respectively. If we only consider cuts where the surface atoms stay threefold coordinated, all slabs representing polar surfaces are automatically stoichiometric and are inevitably Zn terminated

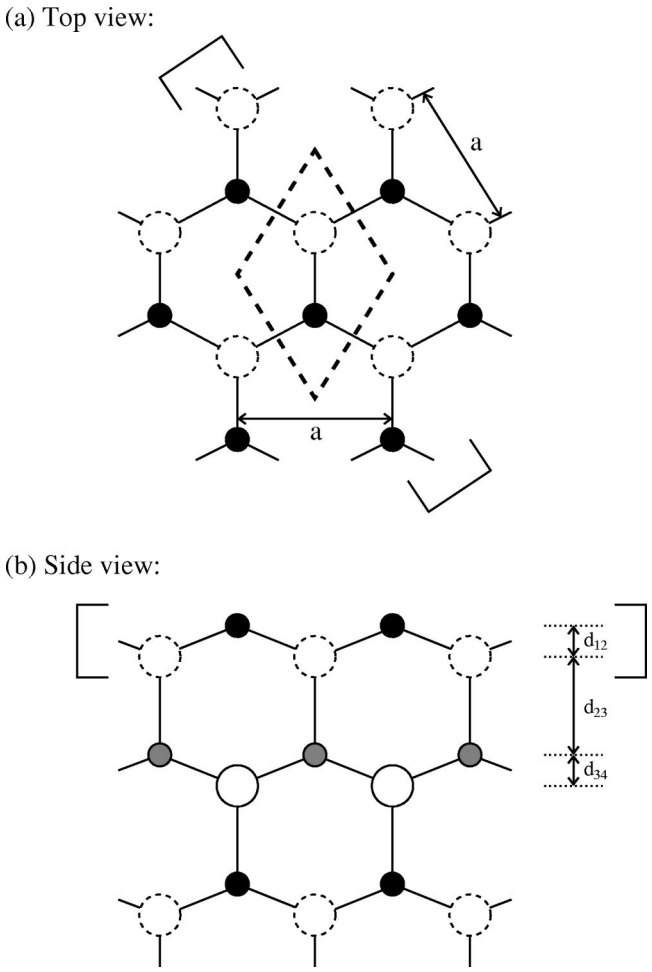

FIG. 4. Schematic top and side view of the polar Zn-terminated (0001) surface. The same representation as in Fig. 2 is used.

on one side and O terminated on the other side. Figure 4 sketches the characteristic sequence of Zn-O double layers of the polar slabs. In our calculations, slabs with 4–20 Zn-O double layers were used, thus containing 8–40 atoms. k-point convergence was achieved with a $(6\times6\times1)$ Monkhorst-Pack[51] grid, and tests with up to $(12\times12\times1)$ k points were made.

Each Zn-O double layer in Fig. 4 exhibits a dipole moment perpendicular to the surface. If we assume for simplicity a purely ionic model for ZnO and assign the fixed formal charges $+Ze$ and $-Ze$ to the Zn and O ions, respectively, then a slab of N double layers will exhibit a dipole moment of $m=NZe(1-2u)c/2$ (see Fig. 5). This corresponds to a spontaneous polarization of $P_s=Ze(1-2u)$, which is independent of the thickness of the slab. If the external electric field is zero, inside the slab an electric field of $E=-4\pi P_s$ will be present. Therefore, no matter how thick we choose our slab, the inner part will *never* become bulklike, and the surface energy, defined as the difference between the energy of the slab and the energy of the same number of atoms in the bulk environment, will *diverge* with slab thickness.[26] Thus, the polar surfaces are *not stable*.

On the other hand, it can easily be seen that if we modify the charge in the top and bottom layer of the slab from $\pm Ze$ to $\pm(Z-\delta)e$ with $\delta=(1-2u)\,Z\approx Z/4$, then the dipole moment of the slab will become *independent* of the slab thickness and the internal electric field *vanishes*. This charge transfer is equivalent to applying an external dipole, which compensates the internal electric field.

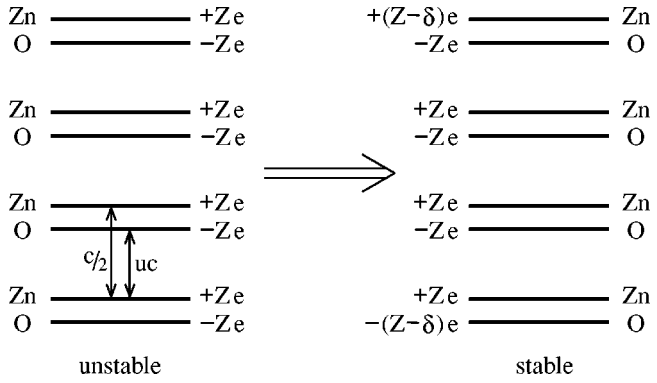

FIG. 5. Schematic illustration of the stacking sequence of the polar slabs. A charge transfer of $\delta=(1-2u)Z\approx Z/4$ has to occur to stabilize the polar surfaces.

For most polar surfaces the rearrangement of the charges is accomplished by a modification of the surface layer composition with respect to the bulk. If this does not occur, the internal electric field will ''tilt'' the band structure, by which the upper edge of the valence band close to the O-terminated surface will become higher in energy than the lower edge of the conduction band at the Zn-terminated face (see Fig. 6). The slab can now lower its energy (thereby reducing the internal electric field) by transferring electrons from the valence band at the O-terminated side to the conduction band at the Zn-terminated face. This will happen ''automatically'' in any self-consistent electronic structure calculation that makes use of a slab geometry. This is what is usually referred to as ''the metallization of polar surfaces.''

However, one problem still remains: electrons move from the O- to the Zn-terminated surface until the upper valence-band edge at the O-terminated side has reached the same energy as the lower edge of the conduction band at the Zn-terminated face as sketched in Fig. 6. In this situation, the internal electric field is not *fully* removed for a finite slab with thickness D. The residual electric field depends on the band gap and vanishes only with $1/D$. In our calculations we

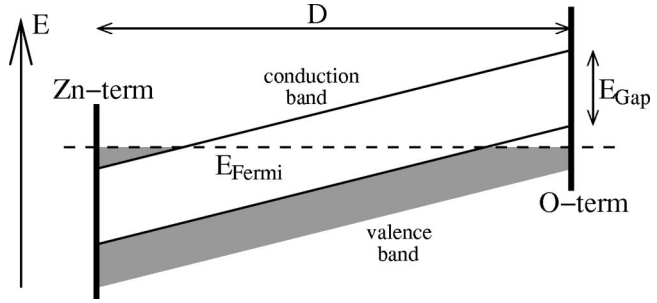

FIG. 6. Schematic illustration of the band structure after electrons have moved from the O- to the Zn-terminated surface of the slab. Depending on the band gap and the thickness D of the slab, a residual electric field remains inside the slab.

found that for slabs with up to six Zn-O double layers, the residual electric field is still so strong that the slabs are not stable. There is no energy barrier when the O and Zn layers are shifted simultaneously and rigidly toward each other. Therefore, to get good converged results for the surface geometries and energies, very thick slabs have to be used, which makes the investigation of the polar surfaces computationally very demanding. Ideally, one should calculate all quantities of interest for different slab thicknesses D and extrapolate the results to $1/D \rightarrow 0$. In the present study we obtained the relaxations of the surface layers (see Fig. 9) as well as the cleavage energy of the polar surfaces (see Fig. 10) by extrapolating the results of slab calculations containing up to 20 Zn-O double layers.

III. RESULTS AND DISCUSSION

A. The nonpolar $(10\bar{1}0)$ and $(11\bar{2}0)$ surfaces

The nonpolar wurtzite $(10\bar{1}0)$ surface and the closely related zinc-blende (110) surface have been studied experimentally and theoretically for a wide range of III-V and II-VI compound semiconductors. It was found that all surfaces show the same basic relaxations with the surface cation moving inwards and the anion staying above, resulting in a tilt of the surface anion-cation dimers, and the magnitude of the relaxation is determined by a competition between dehybridizaton and charge-transfer effects.[21,53–57]

At the surface [this applies also to the $(11\bar{2}0)$ surface], the coordination of the surface atoms is reduced from fourfold to threefold, thereby creating an occupied dangling bond at the anion and an empty dangling bond at the cation. Two limiting cases may now be distinguished: In a dominantly covalent bonded compound the cation will rehybridize from sp^3 to sp^2 and will move downwards until it lies nearly in the plane of its three anion neighbors. The anion stays behind (often even an outward relaxation is observed) tending toward p-like bonds to its neighbors. The result is a strong tilt of the surface anion-cation dimer (up to 30° is observed) with only a small change of the bond length. In a dominantly ionic solid, electrostatics prevails over dehybridization effects. To obtain a better screening, both, anion and cation, move toward the bulk. The tilt of the anion-cation dimer will be small but the bond length can be significantly reduced. Therefore, the relaxation of the surface dimers directly reflects the covalency or ionicity of the chemical bond in the compound of consideration.

Our results for the relaxation of the $(10\bar{1}0)$ surface are given in Tables II and III. All lengths are expressed as fractions of the theoretical lattice parameters given in Table I. Using these dimensionless relative quantities, no significant differences between the LDA and GGA calculations can be seen. For two structural parameters, the decay of the surface relaxations into the bulk is illustrated in Fig. 7. Compared to the topmost surface layer, the tilt angle ω and the in-plane bond-length contraction $C_{B,\|}$ of the Zn-O dimers are already much smaller in the second and the subsequent layers, but still significant deviations from the bulk structure can be seen as deep as five or six layers below the surface.

TABLE II. Summary of the structural relaxations of the first two surface layers for the nonpolar $(10\bar{1}0)$ and $(11\bar{2}0)$ surfaces. The definitions of the independent structural parameters are shown in Figs. 2 and 3. All relaxations are given in fractions of the theoretical bulk lattice constants a and c (see Table I). The rows labeled ''Bulk'' are the corresponding values for the unrelaxed surface.

	$(10\bar{1}0)$ surface		$(11\bar{2}0)$ surface	
	LDA	PBE	LDA	PBE
$\Delta_{1,\perp}$	$+0.106a$	$+0.100a$	$+0.076a$	$+0.073a$
$\Delta_{2,\perp}$	$-0.041a$	$-0.038a$	$-0.016a$	$-0.015a$
Bulk	0.0		0.0	
$\Delta_{1,y}$	$0.6531c$	$0.6539c$	$0.6506c$	$0.6516c$
$\Delta_{2,y}$	$0.6243c$	$0.6231c$	$0.6230c$	$0.6221c$
Bulk	$(1-u)c$		$(1-u)c$	
$\Delta_{1,x}$			$0.083a$	$0.077a$
$\Delta_{2,x}$			$0.020a$	$0.016a$
Bulk			0.0	
$d_{12,\perp}$	$0.1445a$	$0.1447a$	$0.4093a$	$0.4089a$
$d_{23,\perp}$	$0.6328a$	$0.6337a$	$0.5215a$	$0.5222a$
Bulk	$\frac{\sqrt{3}}{6}a$ / $\frac{\sqrt{3}}{3}a$		$a/2$	
$d_{12,y}$	$0.5355c$	$0.5357c$	$0.5259c$	$0.5266c$
$d_{23,y}$	$0.5013c$	$0.5017c$	$0.5014c$	$0.5009c$
Bulk	$c/2$		$c/2$	
$d_{1,x}$			$0.4381a$	$0.4399a$
$d_{2,x}$			$0.5515a$	$0.5556a$
Bulk			$\frac{\sqrt{3}}{3}a$	

The relatively small angle of $\omega \approx 10°$ for the tilt of the surface Zn-O dimer together with the Zn-O bond contraction of $C_{B,\|} \approx 7\%$ confirms that the chemical bond in ZnO is highly ionic, but with significant covalent contributions. A tilt of 10° is at the lower boundary of what has been observed for other III-V and II-VI compounds.[55] Only the ni-

TABLE III. Tilt angle ω of the surface dimer (see Fig. 2) and relative bond-length contraction C_B (in % of the corresponding bulk value) of the surface bonds for the nonpolar $(10\bar{1}0)$ surface, in comparison with LEED experiment and previous calculations. $C_{B,\|}$ refers to the Zn-O dimer bond parallel to the surface, $C_{B,Zn}$ to the back bond of zinc to oxygen in the second layer, and $C_{B,O}$ to the respective back bond of the surface O atom. Bulk values of the surface and back bonds are uc and $[(1/2-u)^2+a^2/3c^2]^{1/2}c$, respectively. pw indicates a plane-wave calculation and ''Gauss'' a calculation employing Gaussian orbitals.

	ω	$C_{B,\|}$	$C_{B,Zn}$	$C_{B,O}$
LDA, this study	10.7°	−6.7	−2.8	−3.2
PBE, this study	10.1°	−7.2	−3.1	−3.5
LEED, Ref. 5	$12° \pm 5°$	-3 ± 6		
LDA+pw, Ref. 21	11.7°	−6.0		
LDA+Gauss, Ref. 18	3.6°	−7.9	−5.2	−2.7
HF, Ref. 19	2.3°	−7.2	−3.6	−3.4
B3LYP, Refs. 20 and 52	5.2°	−4.9	−2.9	−0.5

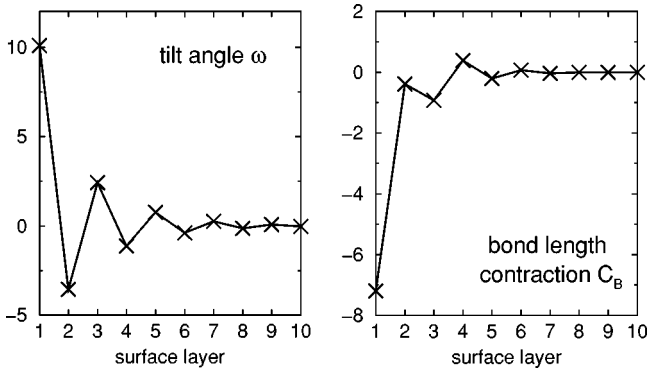

FIG. 7. Deep-layer relaxations for the nonpolar $(10\bar{1}0)$ surface calculated with a 20-layer slab. Plotted are the tilt angle ω (in degrees) and the in-plane bond-length contraction $C_{B,\|}$ (in %) of the Zn-O dimers as a function of the distance from the surface. Only the PBE results are shown, the results from the LDA calculations are essentially identical.

tride semiconductors show tilt angles that are similarly small.[21]

The calculated surface relaxations in Tables II and III agree very well with the DFT-LDA study of Ref. 21 and with the results from the LEED analysis.[5] Relative to the central layer of the slab we find a downward relaxation of the surface atoms of $\Delta d_\perp(\mathrm{Zn}) = -0.36$ Å and $\Delta d_\perp(\mathrm{O}) = -0.04$ Å with a shift parallel to the surface of $\Delta d_\parallel(\mathrm{Zn}) = 0.18$ Å compared to $\Delta d_\perp(\mathrm{Zn}) = -0.45 \pm 0.1$ Å, $\Delta d_\perp(\mathrm{O}) = -0.05 \pm 0.1$ Å, and $\Delta d_\parallel(\mathrm{Zn}) = 0.1 \pm 0.2$ Å from the LEED experiment.

Rotation angles of $\omega = 2° - 5°$ seem anomalously small in the context of what is known for other compounds. Even for the very ionic AlN, a tilt angle of $\omega = 7.5°$ has been reported.[21] The smaller relaxations obtained in Refs. 18–20 may be due to not fully converged calculations. Very thin slabs were partly used or only the first one or two surface layers were relaxed. In Ref. 20 no relaxation of the Zn ions parallel to the surface was allowed. Also the convergence of the localized basis sets employed in these studies and the *k*-point sampling may have been a problem. As a test we made a slab calculation where we fixed the positions of the atoms at the bulk positions and allowed only the first surface layer to relax. The tilt angle ω then reduces to roughly half of its value. Also coarsening the *k*-point mesh from $(4\times2\times2)$ to $(2\times2\times2)$ results in changes of $2° - 3°$ in ω. Since we performed our calculations with two very different pseudopotential approaches we can exclude any bias caused by the use of pseudopotentials.

Tables II and IV show our results for the relaxation of the $(11\bar{2}0)$ surface. The atomic displacements are of the same order of magnitude as has been found for the $(10\bar{1}0)$ surface. Again, no significant differences between the LDA and GGA calculation can be seen. The tilt of the surface dimers of 7.5° and the reduction of the Zn-O dimer bond length of about 6% fits nicely into the picture of ZnO being at the borderline between ionic and covalent solids.

In a hybrid B3LYP study[22] much smaller relaxations for the $(11\bar{2}0)$ surface were reported. However, in this study only three degrees of freedom per surface layer were relaxed. The authors claimed that the position of the Zn and O ions are constrained by symmetry. This is not correct. From the two Zn-O dimers in each surface layer, the atoms of one dimer can move freely in all three Cartesian directions, leading to six degrees of freedom per surface layer (see Fig. 3). The position of the second dimer is then determined by the glide plane symmetry (see also Ref. 54).

TABLE IV. Tilt angle ω of the surface dimer (see Fig. 3) and relative bond-length contraction C_B of the surface bonds for the nonpolar $(11\bar{2}0)$ surface. The same notation as in Table III is used.

	ω	$C_{B,\|}$	$C_{B,Zn}$	$C_{B,O}$
LDA, this study	7.6°	−5.8	−1.4	−1.7
PBE, this study	7.4°	−6.4	−1.5	−1.8

B. The polar (0001)-Zn and $(000\bar{1})$-O surfaces

In Fig. 8 we show the convergence of the relaxation of the topmost surface layers for the polar (0001)-Zn and $(000\bar{1})$-O surfaces depending on the *k*-point mesh and the plane-wave energy cutoff. For a $(6\times6\times1)$ Monkhorst-Pack mesh and a cutoff energy of 20 Ry, well-converged results are obtained, and we have kept those settings for all further calculations. The calculated interlayer distances for the two polar surfaces

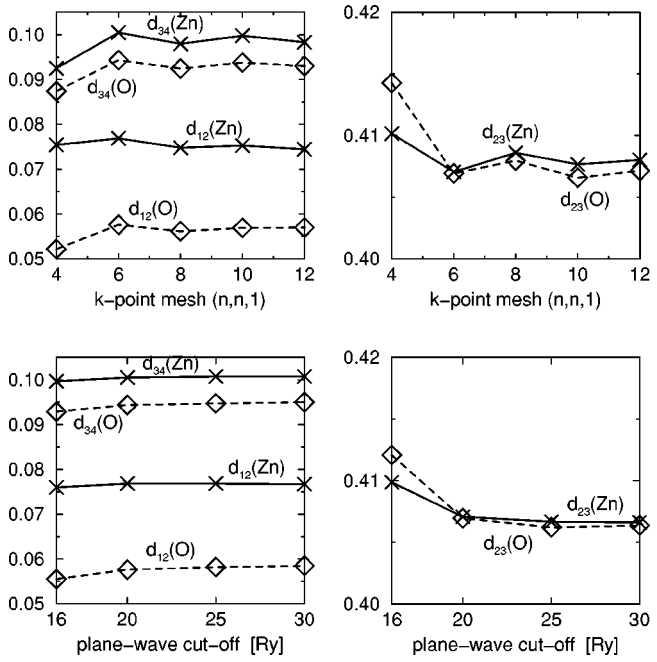

FIG. 8. Convergence of the first three interlayer distances (see Fig. 4) for the polar (0001)-Zn and the $(000\bar{1})$-O surface with respect to *k*-point sampling (top) and plane-wave energy cutoff (bottom). Slabs with eight Zn-O double layers and the PBE functional were used. The *k*-point test was done with a plane-wave cutoff of 20 Ry, and a $(6\times6\times1)$ *k*-point mesh was used for the energy cutoff test. All distances are given in fractions of the theoretical bulk lattice constant *c* (see Table I).

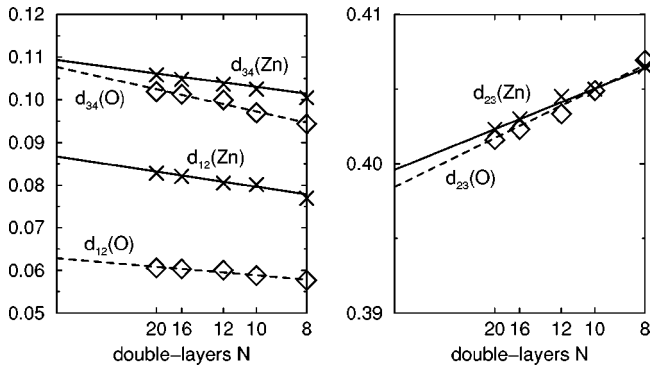

FIG. 9. First three interlayer distances (see Fig. 4) for the polar (0001)-Zn and the $(000\bar{1})$-O surface calculated with different slabs containing N Zn-O double layers and using the PBE functional. All distances are given in fractions of the theoretical bulk lattice constant c (see Table I) and are plotted vs $1/N$. The extrapolation $1/N \rightarrow 0$ gives the surface relaxations for a vanishing internal electric field.

as a function of slab thickness D are plotted in Fig. 9. As expected from the thickness dependence of the residual electric field inside the slab, the $1/D$ plots reveal a nice linear behavior for the interlayer distances. By extrapolating $1/D \rightarrow 0$, all distances may now be obtained in the limit of a vanishing internal electric field.

The extrapolated results for the relaxations of the polar surfaces are summarized in Tables V and VI. Very good agreement with the results of previous *ab initio* calculations is found. In general, all double layers are contracted and the distances between the double layers are increased relative to the bulk spacings. For finite slabs, the residual internal electric field further amplifies this characteristic relaxation pattern.

The largest relaxation is found for the O-terminated surface, where the outermost double-layer distance is compressed by roughly 50%. This agrees reasonably well with the results of the x-ray experiments,[27,32,35] where contractions of 40%, 54%, and 20% were found. On the other hand, from LEED analysis[7] and LEIS measurements[33] it was concluded that the Zn-O double-layer spacing for the O-terminated surface is close to its bulk value. The recent finding of Kunat *et al.*[9] may perhaps help to solve this contradiction. With He scattering it was shown that after commonly used preparation procedures the O-terminated surfaces are usually hydrogen covered. To test how much hydrogen may influence the surface relaxations, we repeated a calculation where we adsorbed hydrogen on top of the O-terminated side of the slab. We find that in this case the outermost Zn-O double-layer expands again, and the Zn-O separation goes back close to the bulk distance. A similar result was also reported by Wander and Harrison.[58]

TABLE V. Summary of the surface relaxations for the polar Zn-terminated (0001)-Zn and the O-terminated $(000\bar{1})$-O surface, (see Fig. 4). All distances are given in fractions of the theoretical bulk lattice constant c (see Table I).

	(0001)-Zn surface		$(000\bar{1})$-O surface	
	LDA	PBE	LDA	PBE
d_{12}	0.0924	0.0867	0.0640	0.0628
d_{23}	0.3958	0.3996	0.3962	0.3985
d_{34}	0.1106	0.1093	0.1079	0.1077
d_{45}	0.3860	0.3889	0.3809	0.3813
d_{56}	0.1148	0.1134	0.1215	0.1221
Bulk	$(\frac{1}{2}-u)c/uc$		$(\frac{1}{2}-u)c/uc$	

TABLE VI. Relaxation of the surface layers of the polar ZnO surfaces in comparison with previous *ab initio* calculations.

	(0001)-Zn surface		$(000\bar{1})$-O surface	
	Δd_{12}	Δd_{23}	Δd_{12}	Δd_{23}
LDA, this study	−24%	+4.6%	−47%	+4.7%
PBE, this study	−28%	+5.4%	−48%	+5.1%
B3LYP, Ref. 27	−23%	+3.5%	−41%	+3.0%
GGA, Ref. 28	−31%	+7.0%	−52%	+6.5%
GGA, Ref. 8	−25%		−41%	

For the Zn-terminated surface there is a clear discrepancy between theory and experiment. All calculations predict consistently a contraction of the first Zn-O double layer of 20–30%, whereas in experiment no contraction[30] or even an outward relaxation of the topmost Zn layer is found.[31,32] This may indicate that the metallization used in all theoretical studies is not the adequate model to describe the polar Zn-terminated surface. Recently Dulub *et al.*[59] proposed a new stabilization mechanism for the Zn-terminated surface. With scanning tunneling microscopy (STM) they found that many small islands with a height of one double layer and many pits one double-layer deep are present on the (0001)-Zn surface. Assuming that the step edges are O terminated, an analysis of the island and pit size distribution yielded a decrease of surface Zn concentration of roughly 25%. Such a reduction of Zn atoms at the surface would be enough to accomplish the charge transfer needed to stabilize the polar surface. It would not be in contradiction with the observed $p(1\times1)$ LEED pattern, since a long-range correlation between the different terraces remains. The missing of 25% of the Zn atoms was also obtained by Jedrecy *et al.*[32] as the best fit of their GIXD data.

A structure where the surface is stabilized by many small islands and pits with a Zn deficiency at the step edges is, of course, far away from the model of a clean, perfectly ordered (0001)-Zn surface, used in the theoretical calculations. Basically all surface Zn atoms will be next to a step edge, and therefore very different relaxations may occur. Unfortunately, it is presently out of the reach of our *ab initio* method to do calculations on slabs representing such an island and pit structure.

For the O-terminated surface, on the other hand, the STM measurements[59] show a very different picture. Smooth and flat terraces separated mostly by a two-double-layer step are observed. The number of single double-layer steps was by far not large enough to account for a similar stabilization mechanism as for the Zn-terminated surface.

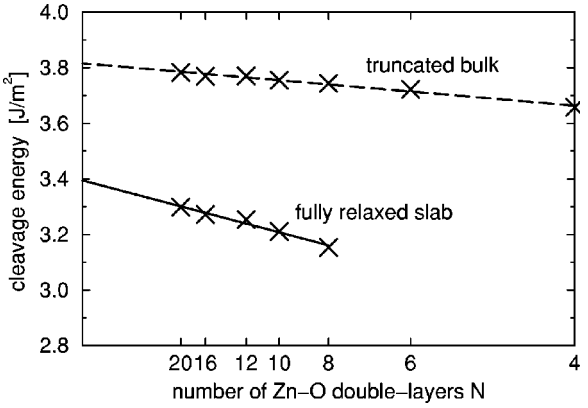

FIG. 10. Similar plot as Fig. 9 for the cleavage energy of the polar ZnO surfaces. Shown are the results of the PBE calculations.

C. Surface/cleavage energies

For the nonpolar surfaces we can obtain directly the surface energy from our slab calculations, since the slabs are always terminated by the same surface on both sides. This is not possible for the polar surface since inevitably both surface terminations are present in a slab calculation. Only the cleavage energy of the crystal is well defined. To be able to compare the relative stability of the nonpolar and polar surfaces, we will discuss in the following only the cleavage energies. The surface energies of the nonpolar surfaces are given by half of their cleavage energy.

Like the interlayer distances, the $1/D$ plot of the cleavage energy for the polar surfaces in Fig. 10 exhibits a simple linear behavior. As can be seen, the cleavage energy does not change too much with the slab thickness, so that moderate slab sizes would be sufficient to obtain reasonable converged results.

The extrapolated values for the cleavage energy of the polar surfaces together with the results for the nonpolar faces and the findings of previous studies are summarized in Table VII. The nonpolar $(10\bar{1}0)$ surface is the most stable face of ZnO with the lowest cleavage energy. But the energy of the $(11\bar{2}0)$ surface is only slightly higher. The cleavage energy for the polar surface is roughly a factor of 2 larger than for the nonpolar surfaces. This is surprisingly low compared to what has been found in other systems, for example, MgO, where a metallization was also assumed as the stabilization mechanism for the polar surfaces.[60] Therefore, for ZnO the metallization mechanism can well compete with other stabilization mechanisms such as reconstructions or randomly distributed vacancies and cannot be ruled out by energetic considerations alone. The LDA and GGA results in Table VII show the same ordering for the cleavage energies of the different surfaces. However, the absolute GGA energies are roughly 30% lower than the LDA results. It is well known that surface energies are usually underestimated in the GGA calculation,[61] and a 30% reduction in the surface energy compared to LDA calculations has also been observed for other metal oxide surfaces.[62] B3LYP partially corrects the GGA deficiency, and, as can be seen in Table VII, B3LYP surface energies are in much better agreement with LDA than GGA results. Overall, our calculated cleavage energies agree very well with previous theoretical results. Interestingly, the relaxation energies are very similar for all surfaces when they are normalized to one Zn-O pair. This means that despite the partially filled bands at the polar surfaces, the strength of the relaxation is almost the same as for the isolating nonpolar faces.

TABLE VII. Cleavage energy E_{cleav} (in J/m^2) and relaxation energy E_{relax} (in eV per surface Zn-O dimer) for the different ZnO surfaces and in comparison with previous calculations.

	E_{cleav}	E_{relax}
$(10\bar{1}0)$ surface		
LDA, this study	2.3	0.37
PBE, this study	1.6	0.37
LDA+pw, Ref. 21	1.7	0.37
B3LYP, Ref. 20 + 27	2.3	
HF, Ref. 19	2.7	0.38
Shell model, Ref. 17	2.0	
$(11\bar{2}0)$ surface		
LDA, this study	2.5	0.29
PBE, this study	1.7	0.30
$(0001)/(000\bar{1})$ surface		
LDA, this study	4.3	0.26
PBE, this study	3.4	0.25
B3LYP, Ref. 27	4.0	

IV. SUMMARY AND CONCLUSIONS

A first-principles density-functional pseudopotential approach was used to determine the fully relaxed atomic structures and the surface/cleavage energies of the nonpolar $(10\bar{1}0)$ and $(11\bar{2}0)$ surfaces and the polar Zn-terminated (0001) and O-terminated $(000\bar{1})$ basal surface planes of ZnO.

The main results of the presented investigation are an extensive set of reliable data for the structural parameters and the energetics of the various ZnO surfaces within the LDA and the PBE approximation, which we consider to be a reference for future studies (see, in particular, the compilations in Tables II, V, and VII).

For the nonpolar surfaces we could resolve the discrepancy between experiment and several previous *ab initio* studies by showing that, if calculations are carefully converged, a moderate tilt of the Zn-O surface dimers with a relatively strong contraction of the dimer bond length is obtained. Such a relaxation pattern is typical for rather ionic compounds, but with a strong covalent contribution to the chemical bonding. Our results are in line with LEED analysis and fit very well the systematic trends that are observed for other more or less ionic II-VI and III-V semiconductors.

The polar surfaces can only be stable if a rearrangement of charges between the Zn- and the O-terminated surfaces takes place. In our calculations the polar surfaces were stabilized by allowing the electrons to move from the $(000\bar{1})$-O to the (0001)-Zn surface, thereby quenching the internal

electric field. Nevertheless, even for thick slabs, a finite residual electric field is present inside the slabs, which affects the results for the structural parameters and surface energy. To get well-converged results in the limit of a vanishing internal electric field, we repeated all calculations with slabs consisting of different numbers of Zn-O double layers and extrapolated the results to the limit of an infinite thick slab.

For both polar surfaces we obtain a strong contraction of the outermost double-layer spacing. This agrees well with experiments for the O-terminated surface but not for the Zn termination, indicating that the electron transfer may not be the adequate model to describe the stabilization mechanism of the polar Zn-terminated surface. Since this is consistently predicted by all calculations, it is very likely that other mechanisms, such as defect formation, hydroxylation, and/or the mechanism proposed by Dulub *et al.*[59] might stabilize the (0001)-Zn surface.

Concerning the surface energies, we find very similar values for the two nonpolar surfaces with a slightly lower value for the $(10\bar{1}0)$ surface. The cleavage energy for the polar surfaces is predicted to be roughly a factor of 2 larger than for the $(10\bar{1}0)$ face.

ACKNOWLEDGMENTS

We wish to thank Volker Staemmler, Karin Fink, and Christof Wöll for fruitful discussions. The work was supported by SFB 558 and FCI.

[1] D.M. Bagnall, Y.F. Chen, Z. Zhu, T. Yao, S. Koyama, M.Y. Shen, and T. Goto, Appl. Phys. Lett. **70**, 2230 (1997).

[2] J. B. Hansen, in *Handbook of Heterogeneous Catalysis*, edited by G. Ertl, H. Knötzinger, and J. Weitkamp (Wiley-VCH, Weinheim, 1997).

[3] P. A. Cox, *Transition Metal Oxides: An Introduction to Their Electronic Structure and Properties* (Clarendon Press, Oxford, 1992).

[4] C.B. Duke, A.R. Lubinsky, S.C. Chang, B.W. Lee, and P. Mark, Phys. Rev. B **15**, 4865 (1977).

[5] C.B. Duke, R.J. Meyer, A. Paton, and P. Mark, Phys. Rev. B **18**, 4225 (1978).

[6] C.B. Duke, J. Vac. Sci. Technol. **14**, 870 (1977).

[7] C.B. Duke and A.R. Lubinsky, Surf. Sci. **50**, 605 (1975).

[8] C. Noguera, J. Phys.: Condens. Matter **12**, R367 (2000).

[9] M. Kunat, St. Gil Girol, Th. Becker, U. Burghaus, and Ch. Wöll, Phys. Rev. B **66**, 081402 (2002).

[10] Several publications (Refs. 13, 17, and 18) quote an earlier LEED analysis of Duke *et al.*, Ref. 4, where a smaller relaxation of the top-layer Zn of -0.3 Å and a larger displacement of O of -0.1 Å was found, leading to a smaller tilt of the Zn-O dimers. As is stated in Ref. 5, Ref. 4 is an analysis of the same experimental data, but the wrong structural bulk model of Ref. 29 was used. Additionally, several conceptual improvements were made in the reanalysis Ref. 5. Under these circumstances, the earlier publication should be disregarded in favor of the results of Ref. 5.

[11] The LEED experiments are sometimes interpreted in literature as concluding that the surface dimer distance is *expanded* compared to the bulk situation (Refs. 13 and 19–21) In these cases, the authors either refer to the older LEED analysis of Ref. 4, or they neglect the lateral displacement $\Delta d_{\parallel}(\mathrm{Zn})$, or misinterpret $\Delta d_{\parallel}(\mathrm{Zn})$ as a shift in the wrong direction. Indeed, the sign convention for the lateral displacements is not very clear in Ref. 5, but from the absolute atomic positions given in the summary of Ref. 5, it becomes clear that Zn relaxes *toward* the O ions, thereby *shortening* the Zn-O distance.

[12] W. Göpel, J. Pollmann, I. Ivanov, and B. Reihl, Phys. Rev. B **26**, 3144 (1982).

[13] N. Jedrecy, S. Gallini, M. Sauvage-Simkin, and R. Pinchaux, Surf. Sci. **460**, 136 (2000).

[14] T.M. Parker, N.G. Condon, R. Lindsay, F.M. Leibsle, and G. Thornton, Surf. Sci. **415**, L1046 (1998).

[15] Y.R. Wang and C.B. Duke, Surf. Sci. **192**, 309 (1987).

[16] I. Ivanov and J. Pollmann, Phys. Rev. B **24**, 7275 (1981).

[17] L. Whitmore, A.A. Sokol, and C.R.A. Catlow, Surf. Sci. **498**, 135 (2002).

[18] P. Schröer, P. Krüger, and J. Pollmann, Phys. Rev. B **49**, 17 092 (1994).

[19] J.E. Jaffe, N.M. Harrison, and A.C. Hess, Phys. Rev. B **49**, 11 153 (1994).

[20] A. Wander and N. M Harrison, Surf. Sci. **457**, L342 (2000).

[21] A. Filippetti, V. Fiorentini, G. Cappellini, and A. Bosin, Phys. Rev. B **59**, 8026 (1999).

[22] A. Wander and N.M. Harrison, Surf. Sci. **468**, L851 (2000).

[23] *Numerical Data and Functional Relationships in Science and Technology*, edited by K.-H. Hellwege and O. Madelung, Landolt-Börnstein, New Series, Group III, Vol. 17, Pt. a and Vol. 22, Pt. a (Springer, New York, 1982).

[24] S.C. Abrahams and J.L. Bernstein, Acta Crystallogr., Sect. B: Struct. Crystallogr. Cryst. Chem. **25**, 1233 (1969); T.M. Sabine and S. Hogg, *ibid.* **25**, 2254 (1969).

[25] C.H. Bates, W.B. White, and R. Roy, Science **137**, 993 (1962); W. Class, A. Ianucci, and H. Nesor, Morelco Rep. **13**, 87 (1966); J.C. Jamieson, Phys. Earth Planet. Inter. **3**, 201 (1970).

[26] P.W. Tasker, J. Phys. C **12**, 4977 (1979).

[27] A. Wander, F. Schedin, P. Steadman, A. Norris, R. McGrath, T.S. Turner, G. Thornton, and N.M. Harrison, Phys. Rev. Lett. **86**, 3811 (2001).

[28] J.M. Carlsson, Comput. Mater. Sci. **22**, 24 (2001).

[29] R. W. G. Wyckoff, *Crystal Structures*, 2nd ed. (Wiley, New York, 1963), Vol. I, pp. 111–112.

[30] M. Sambi, G. Granozzi, G.A. Rizzi, M. Casari, and E. Tondello, Surf. Sci. **319**, 149 (1994).

[31] H. Maki, N. Ichinose, N. Ohashi, H. Haneda, and J. Tanaka, Surf. Sci. **457**, 377 (2000).

[32] N. Jedrecy, M. Sauvage-Simkin, and R. Pinchaux, Appl. Surf. Sci. **162-163**, 69 (2000).

[33] S.H. Overbury, P.V. Radulovic, S. Thevuthasan, G.S. Herman, M.A. Henderson, and C.H.F. Peden, Surf. Sci. **410**, 106 (1998).

[34] M. Galeotti, A. Atrei, U. Bardi, G. Rovida, M. Torrini, E. Zanazzi, A. Santucci, and A. Klimov, Chem. Phys. Lett. **222**, 349 (1994).

[35] N. Jedrecy, S. Gallini, M. Sauvage-Simkin, and R. Pinchaux, Phys. Rev. B **64**, 085424 (2001).
[36] P. Hohenberg and W. Kohn, Phys. Rev. **136**, B864 (1964); W. Kohn and L.J. Sham, *ibid.* **140**, A1133 (1965).
[37] D.M. Ceperley and B.J. Alder, Phys. Rev. Lett. **45**, 566 (1980).
[38] J.P. Perdew and A. Zunger, Phys. Rev. B **23**, 5048 (1981).
[39] J.P. Perdew, K. Burke, and M. Ernzerhof, Phys. Rev. Lett. **77**, 3865 (1996); **78**, 1396 (1997).
[40] D. Vanderbilt, Phys. Rev. B **41**, 7892 (1990).
[41] R.D. King-Smith and D. Vanderbilt, Phys. Rev. B **49**, 5828 (1994).
[42] D. Vanderbilt, Phys. Rev. B **32**, 8412 (1985).
[43] B. Meyer, C. Elsässer, and M. Fähnle, FORTRAN90 program for mixed-basis pseudopotential calculations for crystals, Max-Planck Institut für Metallforschung, Stuttgart.
[44] C.-L. Fu and K.M. Ho, Phys. Rev. B **28**, 5480 (1983).
[45] R.T. Girard, O. Tjernberg, G. Chiaia, S. Söderholm, U.O. Karlsson, C. Wigren, H. Hylén, and I. Lindau, Surf. Sci. **373**, 409 (1997).
[46] D. Vogel, P. Krüger, and J. Pollmann, Phys. Rev. B **54**, 5495 (1996); **52**, R14 316 (1995).
[47] D. Vogel, Dissertation, Universität Münster, Germany, 1998.
[48] W. H. Press, S. A. Teukolsky, W. T. Vetterling, and B. P. Flannery, *Numerical Recipes* (Cambridge University Press, New York, 1986).
[49] L. Bengtsson, Phys. Rev. B **59**, 12 301 (1999).
[50] B. Meyer and D. Vanderbilt, Phys. Rev. B **63**, 205426 (2001).
[51] H. J. Monkhorst and J. D. Pack, Phys. Rev. B **13**, 5188 (1976).
[52] The data given in Ref. 20 is not consistent. In Table III we cite the bond-length values of Table 3, Ref. 20. Using the atomic displacements listed in Table 1, Ref. 20 will lead to different results for the back bond lengths.
[53] M. Lannoo and P. Friedel, *Atomic and Electronic Structure of Surfaces* (Springer-Verlag, Berlin, 1991).
[54] C.B. Duke and Y.R. Wang, J. Vac. Sci. Technol. A **7**, 2035 (1989).
[55] C.B. Duke, J. Vac. Sci. Technol. A **10**, 2032 (1992).
[56] J.P. LaFemina, Surf. Sci. Rep. **16**, 133 (1992).
[57] J. Pollmann, P. Krüger, M. Rohlfing, M. Sabisch, and D. Vogel, Appl. Surf. Sci. **104/105**, 1 (1996).
[58] A. Wander and N.M. Harrison, J. Chem. Phys. **115**, 2312 (2001).
[59] O. Dulub, U. Diebold, and G. Kresse, Phys. Rev. Lett. (to be published); U. Diebold (private communication).
[60] A. Pojani, F. Finocchi, J. Goniakowski, and C. Noguera, Surf. Sci. **387**, 354 (1997).
[61] J.P. Perdew, J.A. Chevary, S.H. Vosko, K.A. Jackson, M.R. Pederson, D.J. Singh, and C. Fiolhais, Phys. Rev. B **46**, 6671 (1992).
[62] J. Goniakowski, J.M. Holender, L.N. Kantorovich, M.J. Gillan, and J.A. White, Phys. Rev. B **53**, 957 (1996).